ISSN 1070-3284, Russian Journal of Coordination Chemistry, 2018, Vol. 44, No. 8, pp. 507–517. © Pleiades Publishing, Ltd., 2018.
Original Russian Text © P. Bourosh, I. Bulhac, O. Covaci, V. Zubareva, T. Mitina, 2018, published in Koordinatsionnaya Khimiya, 2018, Vol. 44, No. 4, pp. 255–265.

Iron(II) Bis-α-Benzyldioximate Complexes with 3- and 4-Pyridine Hemiacetals as Axial Ligands: Synthesis, Structure, and Physicochemical Properties

P. Bourosh[a], *, I. Bulhac[b], O. Covaci[b], V. Zubareva[b], and T. Mitina[b]

[a] *Institute of Applied Physics, Academy of Sciences of Moldova, Chisinau, R. Moldova*

[b] *Institute of Chemistry, Academy of Sciences of Moldova, Chisinau, R. Moldova*

**e -mail: bourosh.xray@phys.asm.md*

Received October 25, 2017

Abstract—The coordination compounds $[Fe(DfgH)_2(HL^1)_2]$ and $[Fe(DfgH)_2(HL^2)_2]$, where DfgH = is the α-benzyldioxime monoanion, HL^1 = 3-pyridine hemiacetals: methoxy(pyridin-3-yl)methanol (**I**), ethoxy(pyridin-3-yl)methanol (**II**); HL^2 = 4-pyridine hemiacetal: methoxy(pyridin-4-yl)methanol (**III**), ethoxy(pyridin-4-yl)methanol (**IV**), and propoxy(pyridin-4-yl)methanol (**V**), were synthesized and studied by X-ray diffraction and IR and Mössbayer spectrosopy. According to X-ray diffration data (CIF files CCDC 1578217–1578221 for **I**–**V**, respectively), all of these Fe(II) complexes are molecular. The metal coordination polyhedron is an octahedron formed by four equatorial nitrogen atoms of two monodeprotonated α-benzyldioxime residues coordinated in the bidentate chelating fashion and by two axial nitrogen atoms of two neutral 3- or 4-pyridine hemiacetal molecules coordinated in the monodentate fashion. The $DfgH^-$ ligands in complexes **I**–**V** are joined by intramolecular O–H···O hydrogen bonds to form a pseudomacrocyclic system. The ligands HL^1 and HL^2 are generated in the reaction of the corresponding alcohols with 3- or 4-pyridinecarboxaldehyde. The IR and Mössbauer spectra of the products were studied. The Mössbauer spectral parameters of compounds **I**–**V** correspond to low-spin iron(II) ions.

Keywords: iron(II) α-benzyldioximates, pyridine hemiacetals, X-ray diffraction, IR spectra, Mössbauer spectra

DOI: 10.1134/S1070328418080018

INTRODUCTION

Iron(II) dioximates with the general formula $[Fe(DioxH)_2L_2]$ (DioxH is α-dioxime monoanion, L are organic neutral monodentate ligands) were synthesized for the first time by L.A. Chugaev [1]. The molecular structure of compounds of this type was first solved by X-ray diffraction for 1,2-cyclohexanedioximates (nioximates) and iron(II) dimethylglyoximates containing imidazole as the axial ligand [2, 3]. When the heme structure was determined [4], it became obvious that iron(II) dioximates can be considered as its simplest models, which stimulated a breakthrough in the synthesis and studies, including X-ray diffraction studies [5], of the coordination compounds of iron with α-dioximes. An important role in the development of this research belongs to Kishinev's scientific school headed by Academician A.V. Ablov, which showed that the Chugaev type Fe(II) compounds with the formula $[Fe(DioxH)_2L_2]$ are octahedral *trans*-dioximates. This was confirmed by known and well studied iron(II) dioximates with different axial ligands and the coordination units containing nitrogen ($FeN_4N'_2$) [1–3, 6–8], carbon (FeN_5C and FeN_4C_2) [9, 10], phosphorus (FeN_4P_2) [11, 12], or arsenic (FeN_4As_2) [13]. Further development of the coordination chemistry of iron(II) complexes with α-dioxime involved extension of the range of Chugaev type complexes via variation of both α-dioximes and axial ligands, including bifunctional ones [6, 14–19], using a variety of physical methods for their characterization. In [20, 21], the synthesis of iron(II) dimethylglyoximate complexes with methyl pyridine derivatives and their first study of Mössbauer spectroscopy were reported. Subsequently, Mössbauer spectroscopy was successfully used to study both iron(II) dioximates [10–14, 18, 22–24] and iron(III) dioximates [25, 26].

Since the attention was focused on models resembling iron porphyrins, i.e., compounds in which the axial ligands are coordinated via nitrogen, the obtained and studied iron dioximates contained pyridine [6, 7], pyrazine [14], β- and γ-picoline [20, 21, 26], imidazole [2, 3], and iso- and nicotinamide [15–17]. Structural studies confirmed the assumptions based on IR spectra [16, 17] about the formation of mononuclear complexes and monodentate coordination of bifunctional axial ligands to the metal via heterocyclic nitrogen. An exception is pyrazine, which acts as a bridging ligand to give a Fe(II) coordination polymer [14]. Iron(II) nioximates containing 3- and 4-pyridinecarboxaldehydes as axial ligands have been described and characterized by elemental analysis and UV spectroscopy [8]. However, it is noteworthy that the mentioned aldehydes are highly reactive, and in an alcohol medium, alcohol molecules add to the aldehyde double bond. This was confirmed by disappearance of the ν(C=O) band from the IR spectrum [27]. No structural information on Fe(II) dioximates containing pyridinecarboxaldehydes is present in the Cambridge Crystallographic Data Centre (CCDC) [5].

The purpose of this study is to prepare Fe(II) α-benzyldioximates with participation of 3- and 4-pyridinecarboxaldehydes and various alcohols as solvents and to study the obtained compounds by various methods, including X-ray diffraction. Five complexes with various 3- and 4-pyridinecarboxaldehyde derivatives, $[Fe(DfgH)_2(HL^1)_2]$ and $[Fe(DfgH)_2(HL^2)_2]$, were prepared, where DfgH is the α-benzyldioxime monoanion; HL^1 is 3-pyridine hemiacetal (methoxy(pyridine-3-yl)methanol (**I**), and ethoxy(pyridine-3-yl)methanol (**II**)); and HL^2 is 4-pyridine hemiacetal (methoxy(pyridine-4-yl)methanol (**III**), ethoxy(pyridine-4-yl)methanol (**IV**), and propoxy(pyridine-4-yl)methanol (**V**)).

EXPERIMENTAL

Synthesis of bis(α-benzyldioximato)di{methoxy-(pyridin-3-yl)methanol}iron(II) (I). A solution of α-benzyldioxime (0.96 g, 4 mmol) and 3-nicotinaldehyde (0.24 mL, 2.5 mmol) in DMF (20 mL) and a solution of sodium acetate trihydrate (0.56 g, 4 mmol) in methanol (20 mL) (for generation of a weakly alkaline medium) were successively added in alternation to a solution of $FeCl_2 \cdot 4H_2O$ (0.40 g, 2 mmol) in methanol (20 mL). Stirring of the resulting solution and generation of inert atmosphere to prevent iron from oxidation were performed by bubbling argon through the reaction mixture, after which the flask with the solution was sealed. After 24 h, crystals suitable for X-ray diffraction were selected from the precipitated product. The rest of the product was washed with methanol and diethyl ether and dried in air. The yield was 0.90 g (55.53% based on $FeCl_2 \cdot 4H_2O$).

For $C_{42}H_{40}N_6O_8Fe$

Anal. calcd., %	Fe, 6.87	C, 62.08	H, 4.96	N, 10.34
Found, %	Fe, 6.67	C, 62.37	H, 5.25	N, 10.52

Synthesis of bis(α-benzyldioximato)di{ethoxy(pyridin-3-yl)methanol}iron(II) (II). (a) The product was prepared similarly to compound **I** with the exception that the reaction was carried out in ethanol and the product was washed with ethanol. The yield was 0.92 g (56.8% based on $FeCl_2 \cdot 4H_2O$).

For $C_{44}H_{44}N_6O_8Fe$

Anal. calcd., %	Fe, 6.64	C, 62.86	H, 5.28	N, 10.00
Found, %	Fe, 6.64	C, 62.59	H, 5.45	N, 10.41

(b) The single crystals of **II** were obtained by adding a solution of α-benzyldioxime (0.24 g, 1.0 mmol) and 3-nicotinaldehyde (0.12 mL, 1.25 mmol) in DMF (5 mL) in alternation with a solution of $CH_3COONa \cdot 3H_2O$ (0.14 g, 1.0 mmol) in ethanol (10 mL) to a solution of $FeCl_2 \cdot 4H_2O$ (0.10 g, 0.5 mmol) in ethanol (10 mL), which was stirred with argon. The flask with the solution thus formed was sealed and placed into a refrigerator. The single crystals were taken out after 24 h.

For $C_{44}H_{44}N_6O_8Fe$

anal. calcd., %	Fe, 6.64	C, 62.86	H, 5.28	N, 10.00
Found, %	Fe, 6.45	C, 62.73	H, 5.17	N, 10.11

Synthesis of bis(α-benzyldioximato)di{me-thoxy(pyridin-4-yl)methanol}iron(II) (III). A solution of α-benzyldioxime (0.96 g, 4 mmol) and 4-pyridinecarboxaldehyde (0.24 mL, 2.5 mmol) in DMF (20 mL) and a solution of $CH_3COONa \cdot 3H_2O$ (0.56 g, 4 mmol) in methanol (20 mL) (for the formation of a weakly alkaline medium) were added in alternation to a solution of $FeCl_2 \cdot 4H_2O$ (0.4 g, 2 mmol) in methanol (20 mL). Stirring of the solution and generation of inert atmosphere to prevent iron from oxidation were performed by bubbling argon through the reaction mixture, after which the flask with the solution was sealed. After 24 h, crystals suitable for X-ray diffraction were selected from the crystalline product. The rest of the product was washed with methanol and diethyl ether and dried in air. The yield was 1.29 g (79.6% based on $FeCl_2 \cdot 4H_2O$).

For $C_{42}H_{40}N_6O_8Fe$

Anal. calcd., %	Fe, 6.87	C, 62.08	H, 4.96	N, 10.34
Found, %	Fe, 6.95	C, 61.87	H, 4.83	N, 10.60

Synthesis of bis(α-benzyldioximato)di{ethoxy(pyridin-4-yl)methanol}iron(II) (IV). (a) The product was prepared similarly to compound **III** with the exception that the reaction was carried out in ethanol and the product was washed with ethanol. The yield was 0.98 g (60.5% based on $FeCl_2 \cdot 4H_2O$).

For $C_{44}H_{44}N_6O_8Fe$

Anal. calcd., %	Fe, 6.64	C, 62.86	H, 5.28	N, 10.00
Found, %	Fe, 6.49	C, 62.59	H, 5.45	N, 10.36

(b) The single crystals of **IV** were obtained by adding a solution of α-benzyldioxime (0.12 g, 0.5 mmol), 4-pyridinecarboxaldehyde (0.06 mL, 0.625 mmol), and $CH_3COONa \cdot 3H_2O$ (0.07 g, 0.5 mmol) in a mixture of DMF (30 mL) and ethanol (15 mL) to a solution of $FeCl_2 \cdot 4H_2O$ (0.05 g, 0.25 mmol) in ethanol (15 mL), which was stirred with argon. The single crystals precipitated after 4 days.

For $C_{44}H_{44}N_6O_8Fe$

Anal. calcd., %	Fe, 6.64	C, 62.86	H, 5.28	N, 10.00
Found, %	Fe, 6.55	C, 62.73	H, 5.17	N, 9.89

Synthesis of bis(α-benzyldioximato)di{propoxy(pyridin-4-yl)methanol}iron(II) (V). A solution of α-benzyldioxime (0.12 g, 0.5 mmol), 4-pyridinecarboxaldehyde (0.06 mL, 0.625 mmol), and $CH_3COONa \cdot 3H_2O$ (0.07 g, 0.5 mmol) in a mixture of DMF (10 mL) and propanol (20 mL) was added to a solution of $FeCl_2 \cdot 4H_2O$ (0.05 g, 0.25 mmol) in DMF (10 mL), which was stirred with argon. The single crystals precipitated on the 5th day.

For $C_{46}H_{48}N_6O_8Fe$

Anal. calcd., %	Fe, 6.43	C, 63.60	H, 5.57	N, 9.68
Found, %	Fe, 6.38	C, 63.42	H, 5.40	N, 9.53

IR spectra were recorded on an Perkin-Elmer Spectrum 100 FT-IR spectrometer in mineral oil mulls for the 4000–400 cm^{-1} range and in the ATR mode in the 4000–650 cm^{-1} range.

Mössbauer spectra were measured on an electrodynamic type setup with a constant acceleration. The ^{57}Co source (1.0 MBq) in the Rh matrix at room temperature was used. The isomer shifts are referred to $Na_2[Fe(CN)_5(NO)] \cdot 2H_2O$. Pellets of finely ground samples of 5–10 mg/cm^2 iron with natural isotope composition served for absorption. The spectra of **II**–**IV** were measured at two temperatures, 300 and 80 K; the spectra of **I** were measured at different temperatures in the 300–5 K range. The simulation of the spectra was performed by the WMOSS (Edina) and WEB Research Co software. The Mössbauer spectral pattern is presented in Fig. 1; isomer shifts and quadrupole splittings are summarized in Table 1.

X-ray diffraction. For single crystals of compounds **I**–**V**, full experimental data were collected at room temperature on an Xcalibur E diffractometer with MoK_α-radiation and graphite monochromator. The crystal structures were solved by direct methods and refined by the least-squares method in the full-matrix anisotropic approximation for non-hydrogen atoms (SHELX-97) [28]. The hydrogen atom positions were calculated geometrically and refined isotropically in the rigid body model with $U_{iso} = 1.2U_{equiv}$ or $1.5U_{equiv}$ of the corresponding O, N, and C atoms. In all structures, the formed –CH(OH)(OR) groups in the axial ligands $HL^{1,2}$ were found to be disordered over two positions.

Crystallographic data and X-ray experiment details for compounds **I**–**V** are summarized in Table 2, selected interatomic distances and bond angles are in Table 3, and the geometric parameters of hydrogen bonds are given in Table 4. The positional and thermal parameters for compounds **I**–**V** are deposited with the Cambridge Crystallographic Data Centre (CCDC) (1578217–1578221, respectively; deposit@ ccdc.cam.ac.uk or http://www.ccdc.cam.ac.uk).

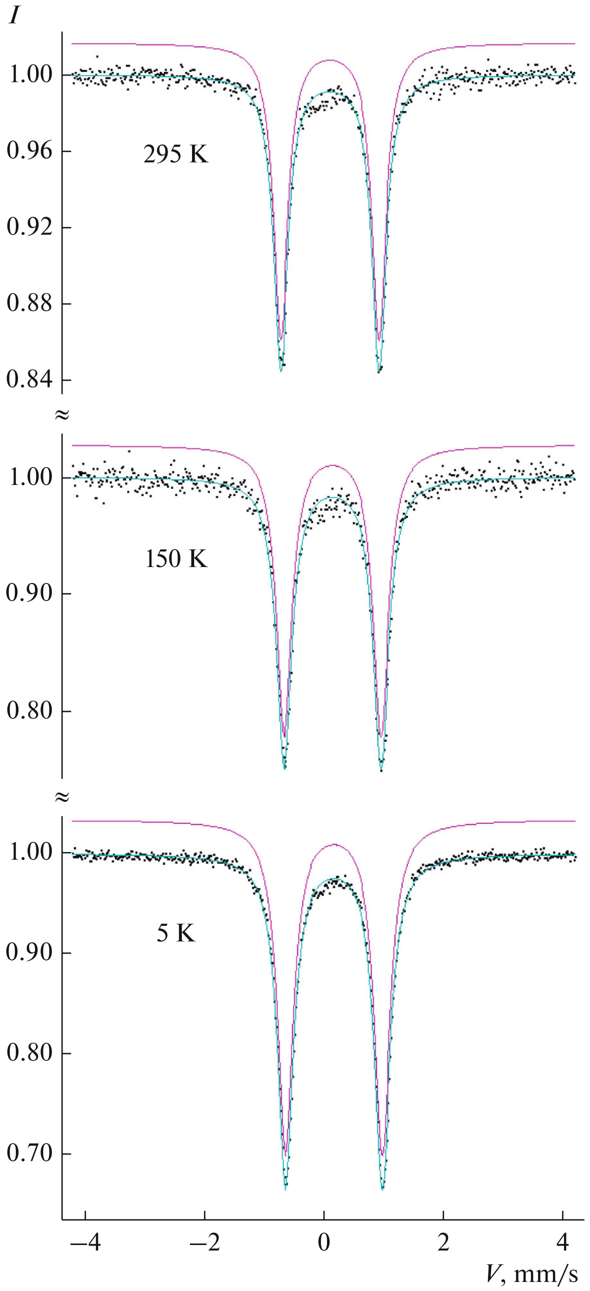

Fig. 1. Mössbauer spectra of complex **I** at different temperatures: continuous line is the simulated spectrum, dashed line is the experimental spectrum.

RESULTS AND DISCUSSION

Compounds **I**–**V** show rather intricate IR spectra with absorption bands corresponding to both coordinated α-benzyldioxime monoanions and hemiacetals

Table 1. Parameters of the Mössbauer spectra of the iron(II) α-benzyldioximates $[Fe(DfgH)_2(HL^{1,2})_2]$*

$HL^{1,2}$	300 K		80 K	
	isomer shift, mm/s	quadrupole splitting, mm/s	isomer shift, mm/s	quadrupole splitting, mm/s
3-CH(OH)OCH_3-Py (**I**)	0.49	1.68	0.47	1.67
3-CH(OH)OC_2H_5-Py (**II**)	0.49	1.71	0.58	1.64
4-CH(OH)OCH_3-Py (**III**)	0.47	1.78	0.55	1.73
4-CH(OH)OC_2H_5-Py (**IV**)	0.49	1.80	0.53	1.68
4-$COOC_2H_5$-Py [15]	0.45	1.92	0.52	1.93
3-$CONH_2$-Py [15]	0.47	1.78	0.52	1.78

* The accuracy of measurement of the isomer shift (δ_{Na^+}) and quadrupole splitting (ΔE_q) is 0.04 mm/s.

generated in the reaction of 3- or 4-pyridinecarboxaldehyde with alcohols during the synthesis of coordination compounds. The IR spectra of the complexes exhibit broad absorption bands at 3400–3030 cm^{-1}, which can be assigned to associated OH groups (ν(OH)) and which partly overlap with ν(CH) of aromatic rings. The 3083–2650 cm^{-1} range contains several narrow bands corresponding to ν(CH) modes; among these, sharp bands at 2739–2722 and 2834–2825 cm^{-1} observed in the spectra of all compounds correspond apparently to the aldehyde ν(CH) modes [27] and to the –O–CH_3-group ν(CH) modes [29], respectively. The bending vibrations of the CH_3 groups occur at 1479–1466 cm^{-1} (δ_{as}) and 1426–1372 cm^{-1} (δ_s). The intense bands in the 1094–1081 cm^{-1} range can be assigned to ν_{as}(–C–O–C) [27]. The relatively broad band at 1663–1654 cm^{-1} is attributable to the ν(C=C) and ν(C=N) modes of aromatic rings. The IR spectra show intense absorption bands for the in-plane and out-of-plane aromatic δ(CH) modes, which characterize the type of substitution in the benzene ring. For complexes with *para*-substituted ligands, $\delta(CH)_{in}$ are at 1124, 1044, and 1039 cm^{-1} and $\delta(CH)_{out}$ are at 833, 796, and 795 cm^{-1}; in the case of *meta*-substitution, $\delta(CH)_{in}$ for three adjacent hydrogen atoms are at 1188, 1177,1088, 1084, 1049, and 1047 cm^{-1} and $\delta(CH)_{out}$ are at 756, 755, 694, and 693 cm^{-1}. The vibrations of the isolated hydrogen atom occur at 878 cm^{-1}. For coordinated $DfgH^-$: $\nu(C{=}N)_{oxime}$, 1505, 1504 cm^{-1}; ν(N–O), 1266–1257 and 1128–1112 cm^{-1}; and $\gamma(OH)_{oxime}$, 933–922 cm^{-1} [11, 13, 18]. For singly substituted α-benzyldioxime benzene rings: $\delta(CH)_{in}$, 1087–1057cm^{-1}; $\delta(CH)_{out,}$ 727–723 and 694–693 cm^{-1} [28, 30]. The bands related to the Fe–N vibrations are recorded at 510–420 cm^{-1}: Fe–N(DfgH), 505, 504 and 438–425 cm^{-1}; Fe–N($HL^{1,2}$), 544–533 cm^{-1} [11, 13, 18].

The Mössbauer spectra of complexes **I**–**IV** in the 300–5 K range are doublets with peaks of approximately equal intensity without additional absorption. A decrease in the temperature to 80 K (or to 5 K in the case of complex **I**) does not change the form of the Mössbauer spectra (Fig. 1). The isomer shifts and quadrupole splittings in the Mössbauer spectra of **I**–**IV** do not depend on temperature and correspond to low-spin ($S = 0$) iron ion in the +2 oxidation state ($\delta_{Na^+} = 0.47$–0.49 mm/s; $\Delta E_Q = 1.68$–1.80 mm/s at 300 K and $\delta_{Na^+} = 0.47$–0.58 mm/s; $\Delta E_Q = 1.64$–1.73 mm/s at 80 K (Table 1) [15, 22].

The structure of compounds **I**–**V** is molecular and is formed by the centrosymmetric $[Fe(DfgH)_2(HL^{1,2})_2]$ complexes. The HL^1 and HL^2 ligands differ in the substituent position in the pyridine ring (3 or 4, respectively) and in the substituent in position 1 of (3- or 4-pyridyl)methane: methoxy in **I** and **III**, ethoxy in **II** and **IV**, and propoxy in **V**. The complexes of pyridine hemiacetals were formed from the corresponding pyridinecarboxaldehydes depending on the solvent used (methanol, ethanol, propanol). Thus, pyridine hemiacetals were generated upon addition of the alcohols to pyridinecarboxaldehydes, although hemiacetals are rarely sufficiently stable. The Fe(II) coordination polyhedron in **I**–**V** is formed by six nitrogen atoms arranged at octahedron vertices, similar to those in the $[Fe(DioxH)_2A_2]$ complexes [2, 3, 6, 7, 14, 15]. The coordination of the Fe central atom in **I**–**V** is formed by two monodeprotonated $DfgH^-$ ligands bound bidentately through two nitrogen atoms and two neutral HL^1/HL^2 ligands bound monodentately through the heterocycle nitrogen (Figs. 2a, 2b). Analysis of CCDC data [5] reveals the complexes of Cu(II)-Hg(II) [30], Pd(II) [31], Mn(III) [32], and Zn(II) [33] with 1-hydroxy-1-methoxy-(4-pyridyl)methane and Ru(II) with its derivative [34], in which this organic ligand is coordinated to metal ions in the monodentate fashion via the nitrogen atom of the aromatic ring.

In compounds **I**–**V**, the Fe(1)–N interatomic distances to the equatorial nitrogen atoms are in the

Table 2. Crystallographic data, X-ray experiment details and structure refinement parameters for complexes **I**–**V**

Compound	**I**	**II**	**III**	**IV**	**V**
M	811.84	840.70	812.65	840.70	868.75
System	Orthorhombic	Orthorhombic	Monoclinic	Monoclinic	Monoclinic
Space group	*Pbca*	*Pbca*	$C2/c$	$C2/c$	$C2/c$
a, Å	20.4721(10)	20.233(1)	18.454(2)	18.88(3)	19.114(2)
b, Å	9.0544(4)	9.2697(6)	12.408(1)	12.13(1)	12.2292(8)
c, Å	20.7710(10)	21.393(2)	19.558(2)	19.82(2)	20.138(2)
β, deg	90	90	116.39(1)	115.3(2)	113.70(1)
V, Å^3	3850.1(3)	4012.3(5)	4011.9(6)	4101(1)	4310.3(7)
Z	4	4	4	4	4
ρ(calcd.), g/cm^3	1.401	1.392	1.345	1.362	1.339
μ, mm^{-1}	0.455	0.439	0.436	0.429	0.411
F(000)	1693	1760	1696	1760	1824
Crystal size, mm	0.40 × 0.12 × 0.10	0.20 × 0.10 × 0.02	0.25 × 0.07 × 0.05	0.10 × 0.04 × 0.02	0.10 × 0.06 × 0.03
θ Range, deg	3.008 – 25.05	2.98 – 25.05	3.28 – 25.50	3.36 – 24.99	3.33 – 25.05
Ranges of reflection indices	$-24 \le h \le 15$, $-10 \le k \le 8$, $-13 \le l \le 24$	$-12 \le h \le 24$, $-10 \le k \le 11$, $-25 \le l \le 24$	$-20 \le h \le 2$, $-15 \le k \le 14$, $-22 \le l \le 23$	$-22 \le h \le 22$, $-10 \le k \le 14$, $-17 \le l \le 23$	$-20 \le h \le 2$, $-13 \le k \le 14$, $-20 \le l \le 23$
Numbers of measured/unique reflections (R_{int})	10471/3408 (0.0340)	8415/3542 (0.1007)	8026/3741 (0.0535)	7100/3580 (0.1752)	9170/3815 (0.0838)
Filling, %	99.9 (θ = 25.05°)	99.7 (θ = 25.05°)	99.8 (θ = 25.50°)	98.6 (θ = 24.99°)	99.7 (θ = 25.05°)
Number of reflections with $I > 2\sigma(I)$	2469	1477	1981	1129	1887
Number of parameters	272	274	264	270	286
GOOF	1.000	0.933	0.968	0.903	0.914
R-factor ($I > 2\sigma(I)$)	$R_1 = 0.0581$, $wR_2 = 0.1402$	$R_1 = 0.0763$, $wR_2 = 0.0731$	$R_1 = 0.0601$, $wR_2 = 0.0603$	$R_1 = 0.0992$, $wR_2 = 0.1452$	$\mathrm{R}_1 = 0.0689$, $wR_2 = 0.0621$
R factor (for the whole array)	$R_1 = 0.0849$, $wR_2 = 0.1514$	$R_1 = 0.2060$, $wR_2 = 0.0940$	$R_1 = 0.1316$, $wR_2 = 0.0714$	$R_1 = 0.2944$, $wR_2 = 0.2053$	$R_1 = 0.1632$, $wR_2 = 0.0769$
$\Delta\rho_{max}/\Delta\rho_{min}$, e Å^{-3}	0.851/–0.337	0.476/–0.290	0.473/–0.302	0.466/–0.714	0.276/–0.301

1.863(7)–1.924(4) range, while the Fe(1)–N distances to the axial nitrogen ligand are in the 1.980(8)–2.013(4) Å range (Table 3). In complexes **I**–**V**, the coordination octahedron of iron is somewhat stretched towards the axial ligands; shortening of the Fe–N(DfgH) bonds can be attributed to the chelation effect. The equatorial plane of complexes **I**–**V** (Figs. 2a, 2b) accommodates the DfgH$^-$ residues coordinated as N,N-type ligands. This gives rise to two chelate metallacycles, with their relative arrangement being stabilized by intramolecular O–H···O hydrogen bonds (Table 4). In coordinated DfgH$^-$, the N–O, C=N, and C–C interatomic distances (Table 3) are close to those found in Fe(II) complexes with monodeprotonated dioximes: α-benzyldioxime and pyridine [6], dimethylglyoxime and imidazole [3], 1,2-cyclohexanedioxime and imidazole [2]. The minor difference between the N(1)–O(1) and N(2)–O(2) interatomic distances in the oxime moieties of the complexes attest to their monodeprotonated state.

The HL^1 or HL^2 molecules, which form the coordination polyhedra of central metal atoms in **I**–**V**, have dihedral angles between the aromatic ring planes and the N$_4$ equatorial planes of 94.3°, 86.7°, 92.2°, 88.5°, and 87.1°, respectively. The relative positions of the DfgH$^-$ and HL ligands in these molecular complexes are stabilized by one (**I**, **II**) or two (**III**–**V**) weak intramolecular C–H···O hydrogen bonds: in **I**, C(35)–H···O(1) ($-x$, $-y$, $-z$) (C···O, 3.292; H···O, 2.60 Å; CHO angle, 131°); in **II**, C(35)–H···O(1) (C···O, 3.259; H···O, 2.58 Å; CHO angle, 131°); in **III**, –C(31)–H···O(1) (C···O 3.307, H···O 2.58 Å, CHO

Table 3. Selected interatomic distances and bond angles in structures **I**–**V**

Bond	*d*, Å				
	I	**II**	**III**	**IV**	**V**
Fe(1)–N(1)	1.919(3)	1.924(4)	1.909(3)	1.863(7)	1.917(3)
Fe(1)–N(2)	1.902(3)	1.910(4)	1.885(3)	1.895(8)	1.890(3)
Fe(1)–N(3)	2.010(3)	2.013(4)	2.011(2)	1.980(8)	2.001(3)
N(1)–O(1)	1.348(4)	1.339(4)	1.342(3)	1.980(8)	1.346(3)
N(2)–O(2)	1.376(3)	1.366(4)	1.386(3)	1.394(8)	1.376(3)
N(1)–C(1)	1.317(4)	1.298(5)	1.317(3)	1.308(9)	1.301(4)
N(2)–C(2)	1.297(4)	1.296(5)	1.295(3)	1.280(9)	1.305(4)
C(1)–C(2)	1.478(5)	1.480(6)	1.475(4)	1.485(10)	1.475(5)
C(36)–O(3)	1.422(6)	1.407(6)	1.358(4)	1.35(1)	1.39(2)
C(36)–O(4)	1.38(2)	1.366(7)	1.384(4)	1.36(1)	1.35(1)
C(37)–O(4)	1.404(7)	1.440(7)	1.416(3)	1.418(10)	1.414(5)
Angle	ω, deg				
	I	**II**	**III**	**IV**	**V**
N(1)Fe(1)N(2)	80.6(1)	80.6(2)	80.16(12)	79.1(3)	80.3(1)
N(1)Fe(1)N(3)	89.6(1)	99.4(2)	99.84(12)	100.9(3)	99.7(1)
N(2)Fe(1)N(3)	90.1(1)	89.6(2)	89.82(10)	89.4(3)	91.1(1)
O(1)N(1)Fe(1)	122.6(2)	90.4(2)	90.18(10)	90.6(3)	88.9(1)
C(1)N(1)Fe(1)	116.7(2)	89.7(3)	87.83(10)	87.7(3)	91.5(1)
O(1)N(1)C(1)	120.6(3)	90.3(2)	92.17(10)	92.3(3)	88.5(1)
O(2)N(2)Fe(1)	124.5(2)	121.8(3)	122.4(2)	121.7(5)	121.5(2)
C(2)N(2)Fe(1)	117.9(2)	116.7(4)	117.2(2)	119.4(6)	116.8(3)
O(2)N(2)C(2)	117.4(3)	121.2(4)	120.4(3)	118.9(6)	121.6(3)
C(31)N(3)Fe(1)	121.7(2)	124.0(3)	122.83(19)	122.9(5)	123.6(2)
C(35)N(3)Fe(1)	121.7(3)	117.3(4)	119.1(2)	120.3(6)	118.6(3)
C(31)N(3)C(35)	116.6(3)	118.4(4)	118.0(3)	116.7(7)	117.8(3)
N(1)C(1)C(2)	112.2(3)	121.6(4)	123.0(2)	121.4(6)	121.1(3)
N(2)C(2)C(1)	112.5(3)	122.5(4)	121.2(2)	122.4(7)	123.2(3)
O(4)C(36)O(3)	112.5(3)	115.8(4)	115.8(3)	115.9(8)	115.6(4)
C(36)O(4)C(37)	114.0(5)	112.6(5)	111.8(3)	111.2(7)	112.9(4)
		112.6(5)	111.6(3)	109.8(7)	111.3(4)
		115.7(6)	115.2(4)	120.4(14)	114.1(10)
		113.3(6)	116.0(3)	114.5(9)	117.0(6)

angle, 136°) and C(35)–H···O(1) ($-x + 1/2$, $-y + 1/2$, $-z + 1$) (C···O, 3.219; H···O, 2.48 Å; CHO angle, 137°); in **IV**, C(31)–H···O(1) (C···O, 3.248; H···O, 2.55 Å; CHO angle, 132°) and C(35)–H···O(1) ($-x + 1/2$, $-y + 1/2$, $-z + 1$) (C···O, 3.259; H···O, 2.57 Å; CHO angle, 131°); in **V**, C(31)–H···O(1) (C···O 3.325, H···O 2.63 Å, CHO angle 132°) and C(35)–H···O(1) ($-x + 1/2$, $-y + 1/2$, $-z$) (C···O, 3.289; H···O, 2.62 Å; CHO angle, 129°). This type of arrangement of DfgH^- and neutral HL^1 or HL^2 ligands was also found in iron(II) complexes with imidazole [2, 3] or pyridine [6] and in iron(III) complexes with β-picoline [26].

Table 4. Geometric parameters of the main intra- and intermolecular hydrogen bonds in structures **I**–**V**

D–H···A contact	Distance, Å			DHA angle, deg	Coordinates of A atoms
	D–H	H···A	D···A		
I					
O(2)–H(1)···O(1)	0.82	1.81	2.598(4)	159	–*x*, –*y*, –*z*
O(3)–H(1)···O(1)	0.82	1.92	2.735(5)	176	–*x* – 1/2, *y* – 1/2, *z*
II					
O(2)–H(1)···O(1)	0.82	1.80	2.583(4)	160	–*x* + 2, –*y*, –*z* + 1
O(3)–H(1)···O(1)	1.05	1.90	2.745(5)	135	*x* + 1/2, –*y* + 1/2, –*z* + 1
O(3*A*)–H(1)···O(1)	0.85	1.93	2.78(2)	180	*x* + 1/2, –*y* + 1/2, –*z* + 1
III					
O(2)–H(1)···O(1)	0.88	1.67	2.549(3)	173	–*x* + 1/2, –*y* + 1/2, –*z* + 1
O(3*A*)–H(1)···O(1)	0.85	1.83	2.684(3)	179	–*x* + 1/2, *y* – 1/2, –*z* + 1/2
O(3*B*)–H(1)···O(1)	0.85	1.96	2.814(9)	179	–*x* + 1/2, *y* – 1/2, –*z* + 1/2
IV					
O(2)–H(1)···O(1)	0.82	1.76	2.548(8)	159	–*x* + 1/2, –*y* + 1/2, –*z* + 1
O(3)–H(1)···O(1)	0.82	1.99	2.704(11)	145	–*x* + 1/2, *y* – 1/2, –*z* + 1/2
O(3*A*)–H(1)···O(1)	0.82	2.14	2.84(2)	142	–*x* + 1/2, *y* – 1/2, –*z* + 1/2
V					
O(2)–H(1)···O(1)	0.82	1.80	2.583(4)	160	–*x* + 2, –*y*, –*z* + 1
O(3)–H(1)···O(1)	1.05	1.90	2.745(5)	135	*x* + 1/2, –*y* + 1/2, –*z* + 1
O(3*A*)–H(1)···O(1)	0.85	1.93	2.78(2)	180	*x* + 1/2, –*y* + 1/2, –*z* + 1

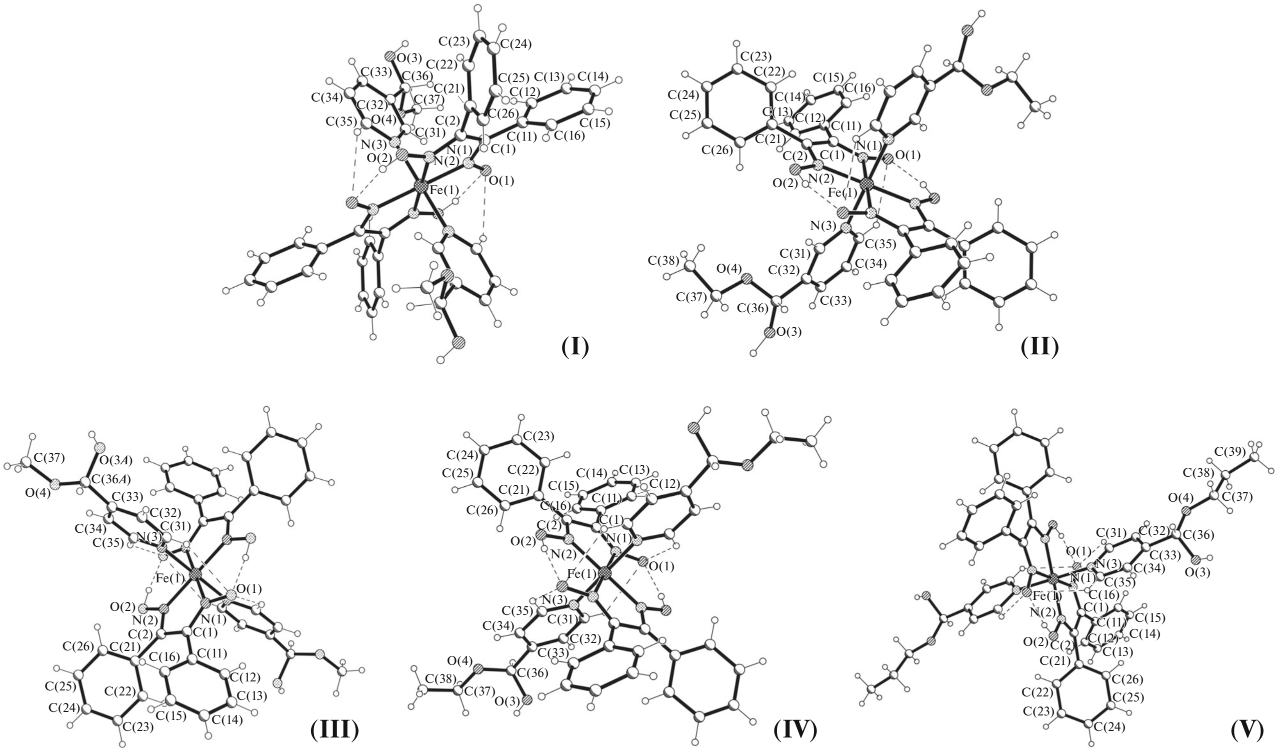

Fig. 2. Molecular structures of **I**–**V** with atom numbering.

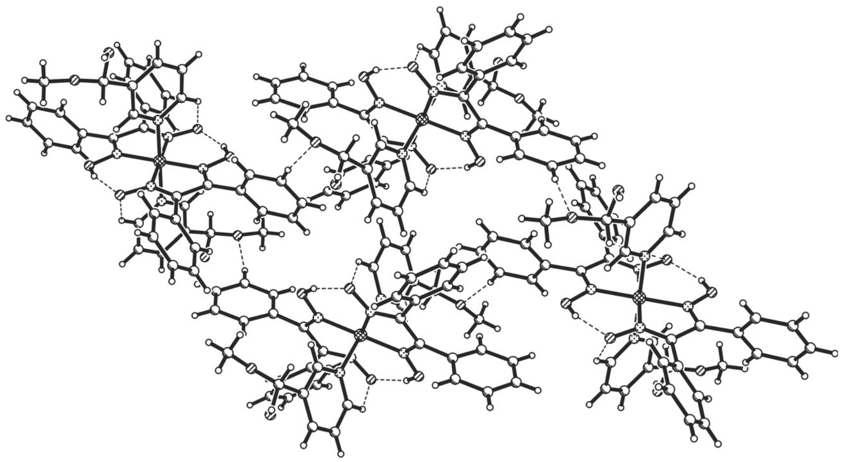

Fig. 3. Fragment of the centrosymmetric layer formed by the intermolecular hydrogen bonds, O(3)–H···O(1) and C(23)–H···O(4), in **I**.

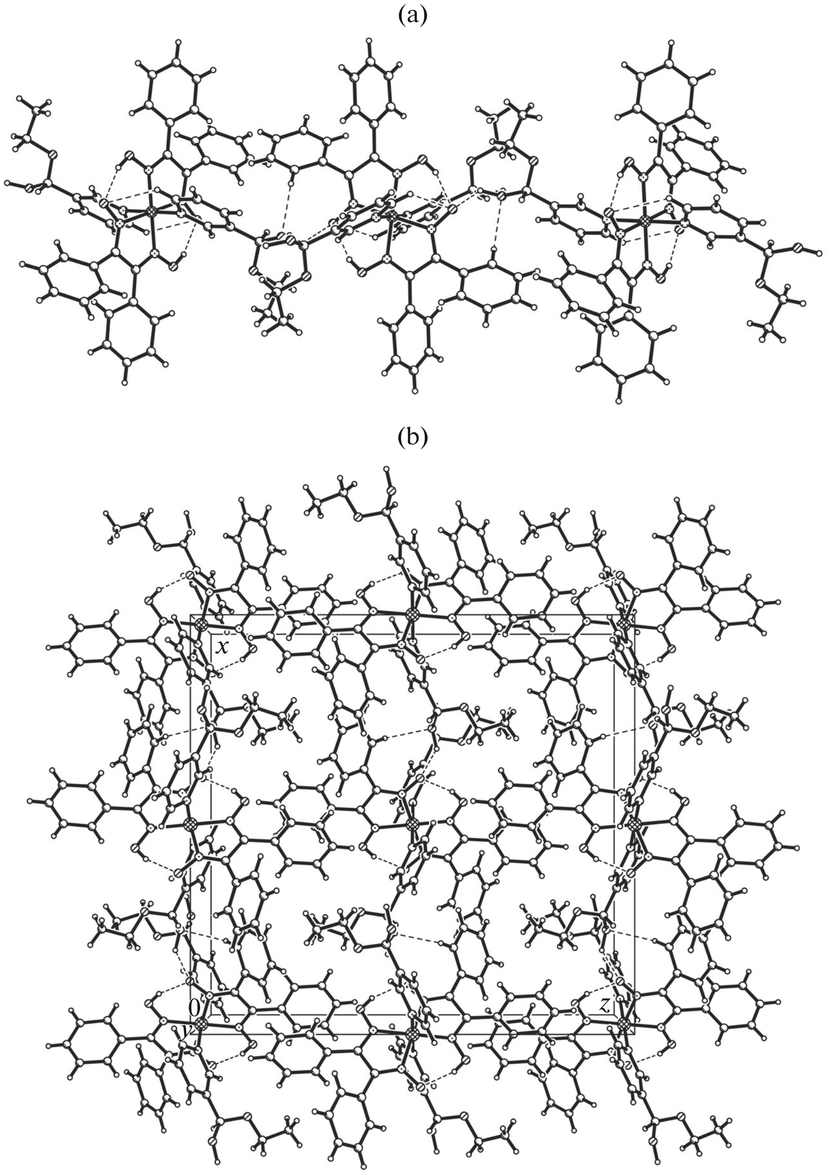

(a)

(b)

Fig. 4. (a) Chain formation from the layer and (b) packing fragment in **II**.

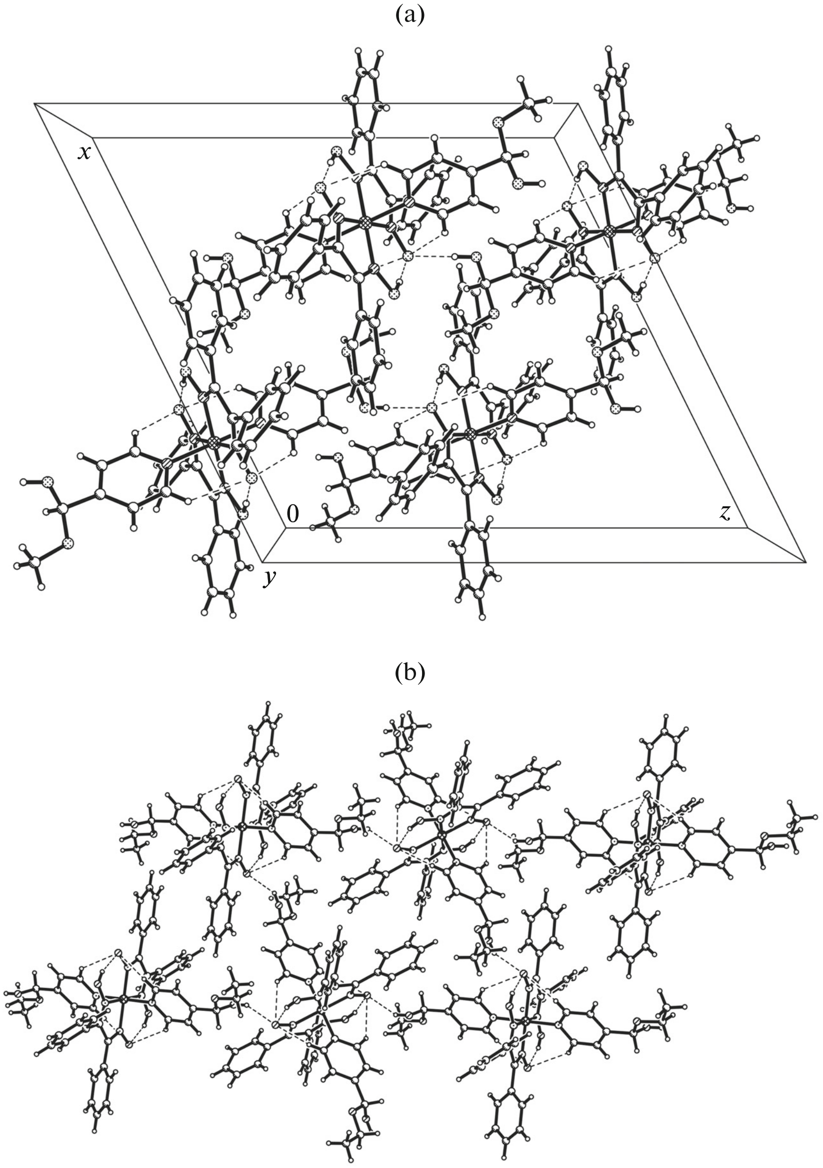

Fig. 5. Formation of the layer by intermolecular O(3)–H···O(1) hydrogen bonds in (a) **III** and (b) **IV**.

The interatomic distances and bond angles for the coordinated HL^1 molecules in **I** and **II** and HL^2 molecules in **III**–**V** do not differ from those found for transition metal complexes with these ligands [30, 31].

In the crystals, complexes **I**–**V** are joined to form centrosymmetric layers by intermolecular O–H···O hydrogen bonds, in which the hydroxyl groups of HL^1 or HL^2 are proton donors and the oxime O atoms are proton acceptors (Table 4). The packing of complexes in these crystals is shown in Figs. 3–6. The crystal structure contains weak intermolecular C–H···O hydrogen bonds, which not only stabilize the layers, but combine them into a three-dimensional framework in **I** and **II**: in **I**, C(12)–H···O(3) ($-x - 1/2$, $y + 1/2$, z) (C···O, 3.013; H···O, 2.54 Å; CHO angle, 149°), C(23)–H···O(4) (x, $-y - 1/2$, $z + 1/2$) (C···O, 3.436; H···O, 2.51 Å; CHO angle, 172°) and C(36)–H···O(3*A*) ($-x - 1/2$, $y + 1/2$, z) (C···O, 3.427; H···O, 2.64 Å; CHO angle, 137°); in **II**, C(16)–H···O(3) ($x - 1/2$, $-y + 1/2$, $-z + 1$) (C···O, 3.338; H···O, 2.50 Å; CHO angle, 150°). Meanwhile, in the crystals of compounds **III**–**V**, no intermolecular C–H···O hydrogen bonds were found. The other intermolecular contacts in these structures correspond to the sums of van der Waals radii of the atoms.

Thus, it was found that the transition metal coordination in compounds **I**–**V** is usual for *trans*-octahedral complexes. The equatorial plane of the coordination polyhedra of metal ions contains two N,N-coordinated α-benzyldioxime residues, which form two five-membered chelate metallacycles, and the axial posi-

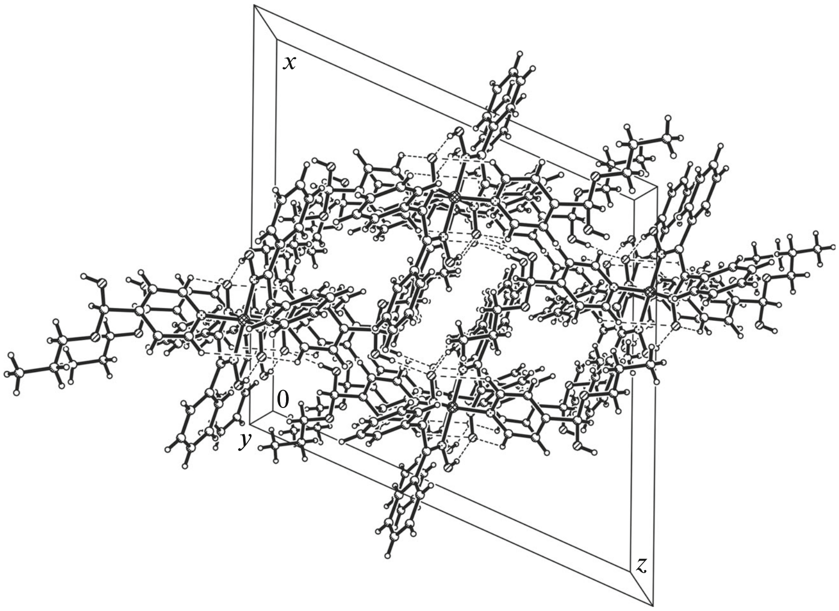

Fig. 6. Fragment of the crystal structure of **V**.

tions are occupied by neutral 3- or 4-pyridine hemiacetal molecules with various substituents coordinated to the central metal atom via nitrogen of the aromatic ring. Probably, the rigid equatorial moiety present in transition metal dioximates, which favors the octahedral coordination of the metal, forces other organic molecules to bind to the metal in the monodentate fashion via the heteroatom of the aromatic ring.

ACKNOWLEDGMENTS

The authors are grateful to G. Filoti (National Institute of Materials Physics, Magurele, Romania) and M. Iacob (Institute of Macromolecular Chemistry, Iasi, Romania) for help in recording the Mössbauer spectra of complex **I** in the 295–5 K range and simulation of Mössbauer spectra.

REFERENCES

1. Chugaev L.A., *Metallicheskie soedineniya α-dioksimov. izbrannye trudy* (Metal Compounds of α-Dioximes. Selected Works), Moscow: Izd. AN SSSR, 1954, vol. 1, p. 56.
2. Prout, C.K. and Wiseman, T.J., *J. Chem. Soc.*, 1964, p. 497.
3. Bowman, K., Gaughan, A.P., and Dori, Z., *J. Am. Chem. Soc.*, 1972, vol. 94, no. 3, p. 727.
4. Perutz, M.F., Rossmann, M.G., Cullis, A.F., et al., *Nature*, 1960, vol. 185, no. 4711, p. 416.
5. Allen, F.H., *Acta Crystallogr., Sect. B: Struct. Sci.*, 2002, vol. 58, nos. 3–1, p. 380.
6. Bulhac, I., Bourosh, P., Bologa, O., et al., *Russ. J. Inorg. Chem.*, 2010, vol. 55, no. 7, p. 1111.
7. Rose, M.J., Gray, H.B., and Winkler, J.R., *J. Am. Chem. Soc.*, 2012, vol. 134, p. 8310.
8. Sanders, N. and Day, P., *J. Chem. Soc. A*, 1969, no. 15, p. 2303.
9. Simonov, Yu.A., Dvorkin, A.A., Bulhac, I.I., et al., *Koord. Khim.*, 1979, vol. 5, no. 12, p. 1883.
10. Turte, K.I., Bulhac, I.I., Starysh, M.P., et al., *Koord. Khim.*, 1980, vol. 6, no. 7, p. 1041.
11. Turte, K.I., Zubareva, V.E., Shafranskii, V.N., et al., *Koord. Khim.*, 1987, vol. 13, no. 5, p. 634.
12. Simonov, Yu.A., Turte, K.I., Bulhac, I.I., et al., *Koord. Khim.*, 1987, vol. 13, no. 3, p. 418.
13. Zubareva, V.E., Turte, K.I., Shafranskii, V.N., et al., *Koord. Khim.*, 1987, vol. 13, no. 8, p. 1067.
14. Kubel, F. and Strahle, J., *Z. Naturforsch., A: Phys. Sci.*, 1983, vol. 38, p. 258.
15. Bulhac, I.I., Bourosh, P.N., Sholmaier, D., et al., *Russ. J. Coord. Chem.*, 2009, vol. 35, no. 5, p. 352.
16. Batyr, D.G. and Bulhacm I.I., *Izv. Akad. Nauk Moldavskoi SSR. Ser. Biol. Khim. Nauk*, 1971, no. 1, p. 77.
17. Batyr, D.G. and Bulhac I.I., *Izv. Akad. Nauk Moldavskoi SSR. Ser. Biol. Khim. Nauk*, 1971, no. 3, p. 71.
18. Bulhac, I.I., Rychagova, I.E., and Zubareva, V.E., et al., *Zh. Neorg. Khim.*, 1990, vol. 35, no. 7, p. 1737.
19. Simonov, Yu.A., Zubareva, V.E., Bulhac, I.I., et al., *Dokl. Akad. Nauk SSSR*, 1986, vol. 287, no. 1, p. 122.
20. Ablov A.V. and Zubarev V.N., *Zh. Neorg. Khim.*, 1973, vol. 18, no. 2, p. 559.
21. Dale, B.W., Williams, R.J.P., Edwards, P.R., et al., *Trans. Faraday Soc.*, 1968, vol. 64, p. 620.

22. Ablov, A.V., Gol'danskii, V.I., Stukan, R.A., et al., *Dokl. Akad. Nauk SSSR*, 1969, vol. 186, pp. 850–853.
23. Turtă, K., Spătaru, T., Bulgac, I., et al., *Rev. Roum. Chim.*, 1994, p. 1035.
24. Bulhac, I.I., Turte, K.I., and Zubareva, V.E., *Koord. Khim.*, 1991, vol. 17, no. 2, p. 243.
25. Turte, K.I., Bulhac, I.I., Zubareva, V.E., et al., *Russ. J. Inorg. Chem.*, 1996, vol. 41, no. 3, p. 516.
26. Dvorkin, A.A., Simonov, Yu.A., Malinovskii, T.I., et al., *Dokl. Akad. Nauk SSSR*, 1977, vol. 234, no. 6, p. 1372.
27. Bellamy, L.J., *The Infrared Spectra of Complex Molecules*, New York: Wiley, 1958.
28. Sheldrick, G.M., *Acta Crystallogr., Sect. A: Found. Crystallogr.*, 2008, vol. 64, no. 1, p. 112.
29. Nakanishi, K., *Infrared Absorption Spectroscopy — Practical*, San Francisco: Holden-Day Inc., 1962.
30. Machura, B., Switlicka, A., Zwolinski, P., et al., *J. Solid State Chem.*, 2013, vol. 197, p. 218.
31. Malecki, J.G. and Zwolinski, P., *Polyhedron*, 2012, vol. 39, p. 85.
32. Ross, I., Euan, B., and White, F., *CSD Communication* (*Private Communication*), 2015.
33. Kalita, A.Ch., Gupta, S.K., and Murugave, R., *Chem.-Eur. J.*, 2016, vol. 22, p. 6863.
34. Bischof, C., Joshi, T., Dimri, A., et al., *Inorg. Chem.*, 2013, vol. 52, p. 9297.

Translated by Z. Svitanko